

MODern River archivES of Particulate Organic Carbon: MOREPOC

Yutian Ke^{1*}, Damien Calmels¹, Julien Bouchez², Cécile Quantin¹

¹ GEOPS, Université Paris-Saclay-CNRS, Orsay, 91405, France

² Université de Paris-Cité, Institut de physique du globe de Paris, CNRS, Paris, 75005, France

* Now at Division of Geological and Planetary Sciences, California Institute of Technology, Pasadena, CA 91125, USA

Correspondence to: Yutian Ke (yutianke@caltech.edu; yutian.ke@universite-paris-saclay.fr)

Abstract. Riverine transport of particulate organic carbon (POC) associated with terrigenous solids to the ocean has an important role in the global carbon cycle. ~~The supply of particulate organic carbon (POC) associated with terrigenous solids transported to the ocean by rivers plays a significant role in the global carbon cycle.~~ To advance our understanding of the source, transport, and fate of fluvial POC from regional to global scales, databases of riverine POC are needed, including elemental and isotope composition data from contrasted river basins in terms of geomorphology, lithology, climate, and anthropogenic pressure. Here, we present a new, open-access, georeferenced, global database called Modern River Archives of Particulate Organic Carbon (MOREPOC) version 1.01, featuring data on POC in suspended particulate matter (SPM) collected at ~~231-233~~ 231-233 locations across ~~118-121~~ 118-121 major river systems. This database includes ~~3,424-546~~ 3,424-546 SPM data entries, among which ~~2,943-3,053~~ 2,943-3,053 with POC content, ~~3,260-402~~ 3,260-402 with stable carbon isotope ($\delta^{13}\text{C}$) values, ~~2,018-283~~ 2,018-283 with radiocarbon activity ($\Delta^{14}\text{C}$) values, ~~1,838-936~~ 1,838-936 with total nitrogen content, and ~~309-299~~ 309-299 with aluminum-to-silicon mass-ratios (Al/Si). The MOREPOC database aims at being used by the Earth System community to build comprehensive and quantitative models for the mobilization, alteration, and fate of terrestrial POC. The database is made available on the Zenodo repository in machine-readable formats as data table and GIS shapefile at <https://doi.org/10.5281/zenodo.7055970> ~~<https://doi.org/10.5281/zenodo.6541925>~~ (Ke et al., 2022).

1. Introduction

Rivers are the main conveyor of terrestrial material to the ocean in the form of suspended particulate matter (SPM), which carries particulate organic carbon (POC) (Leithold et al., 2016; Blair and Aller, 2012). ~~POC is defined as operationally defined as the fraction of total organic carbon contained in the solid fraction recovered after filtration of river water. all combustible, non-carbonate carbon that can be collected on a filter.~~ Before reaching coastal environment and being eventually buried at the ocean bottom, terrestrial POC may experience alteration and/or degradation processes during fluvial transport. ~~The input of terrestrial POC to coastal and ocean environments and alteration in the transport trajectory is a~~ These processes need to be better quantified as they are key features of the global carbon cycle, particularly in the context of current global environmental changes.

Riverine POC is a mixture of organic carbon (OC or C_{org}) from various sources, which can be split into two major origins:

35 biospheric POC (POC_{bio}) and petrogenic POC ($\text{POC}_{\text{petro}}$) (Blair et al., 2003; 2004; Galy et al., 2007; Hilton et al., 2008). Land
Plants, microbes, soils, and aquatic authigenic organisms, and microbes can all contribute radiocarbon-active riverine POC,
with ages ranging from modern to multi-millennial (Galy et al 2007; Blair et al., 2010; Hilton et al., 2011). Radiocarbon-dead
40 $\text{POC}_{\text{petro}}$ is derived from the erosion of sedimentary rocks and consists of terrestrial or marine organic carbon photosynthesized
millions of years ago and have has survived to at least one full erosion/sedimentation/exhumation cycle (Galy et al., 2008a;
Hilton et al., 2011). The balance between the release of CO_2 by oxidation of $\text{POC}_{\text{petro}}$ and the drawdown of CO_2 by burial of
 POC_{bio} in marine sediments controls the impact of the OC cycle on atmospheric CO_2 level at-over geological time-scales (>
100,000 years). The resulting long-term global carbon fluxes are similar in magnitude to those from silicate weathering and
volcanism (Berner, 2003; Hilton et al., 2014; Petsch, 2014; Galy et al., 2007; Galy and Eglinton, 2011; Hilton and West, 2020).
45 Net continental POC_{bio} burial accounts for about 35-70 MtC/yr considering that only 30% of the total riverine input to the
ocean is efficiently buried (Blair and Aller, 2012; Burdige, 2005; Galy et al, 2015), while the oxidation of $\text{POC}_{\text{petro}}$ in
sedimentary rocks would release about 40-100 MtC/yr to the atmosphere (Petsch, 2014; Hilton and West, 2020). These fluxes
are comparable to those induced by silicate weathering, carbonate weathering by oxidation of sulfides, and volcanism,
demonstrating that POC could play an important role in the Earth's long term carbon cycle (Berner, 2003; Hilton et al., 2014;
50 Petsch, 2014; Galy et al., 2007; Galy and Eglinton, 2011; Hilton and West, 2020). Consequently, it is fundamental to quantify
POC sources and fluxes as well as to understand the fate of the different POC pools, in order to better constrain the role that
played by POC plays in the global carbon cycle. To that aim, radiocarbon activity provides unique information on POC age,
residence time, and source. Thanks to improved carbon-dating technology and more easily accessible accelerator mass
spectrometry (AMS, Wacker et al., 2010), routine and high-precision radiocarbon dating has been extensively applied for the
analysis of radiocarbon abundance in riverine POC during the last two decades. Together with the stable isotope composition
of carbon ($^{13}\text{C}/^{12}\text{C}$ ratio, expressed as $\delta^{13}\text{C}$), POC content, or other organic-inorganic proxies (e.g., organic carbon-to-nitrogen
 $\text{C}_{\text{org}}/\text{N}$ ratio, aluminum-to-organic carbon Al/OC ratio), radiocarbon activity helps to constrain the source, transport, and fate
of riverine POC (Raymond and Bauer, 2001).

55 Globally, rivers drain areas of contrasted lithology, climate, tectonics, vegetation, and anthropogenic pressure, parameters that
can all impact riverine POC fluxes. At the global scale, riverine POC_{bio} is known to be dominantly sourced from soil organic
carbon (SOC) (e.g., Tao et al., 2015; Wu et al., 2018; Wild et al., 2019), whose turnover time (the ratio of OC stock to OC
input flux in soil) and thus radiocarbon activity, are greatly controlled by temperature and precipitation (Shi et al., 2020;
Eglinton et al., 2021; Carvalhais et al., 2014). In permafrost regions, SOC has a longer turnover time and is depleted in ^{14}C ,
whereas SOC with the shortest turnover time and the most enriched ^{14}C signature is found in tropical forests and savannahs
60 (Shi et al., 2020; Carvalhais et al., 2014). Consequently, riverine POC is significantly older in Arctic rivers (e.g., Kolyma,
Lena) than in tropical rivers such as the Congo or Amazon (Holmes et al., 2022; Marwick et al., 2015; Mayorga et al., 2005)
due to a major input of aged biospheric OC from thawing permafrost (Wild et al., 2019; Hilton et al., 2015). The geodynamic
setting of a river system also exerts a strong control on POC dynamics. In passive margins, terrigenous sediment typically
experiences a series of erosion-deposition episodes because of the long distances between the upland source region and the

65 ocean (Blair and Aller, 2012). Consequently, it is on active margins that the original POC source signature is transmitted with
the ~~best-greater~~ fidelity (Blair and Aller, 2012). Finally, humans greatly modify the delivery of **fluvial sediment and associated**
POC to the ocean. **In the last decade, sediment delivery in fluvial systems has increased by 215% whereas the net export of**
70 **riverine sediment to the ocean simultaneously decreased by 49% (Syvitski et al., 2022), indicating the changing amount of**
~~eroded POC mobilized to fluvial systems and the final exported POC mass to the ocean (Stallard, 1998).~~~~in particular through~~
~~massive storage of POC at reservoirs (Best et al., 2019; Battin et al., 2009) or a~~ While land-use change (e.g., soil erosion by
agricultural practices) can (Montgomery, 2007; Quinton et al., 2010) lead to increasing terrestrial POC input (Syvitski et al.,
2022; Dethier et al., 2022; Montgomery, 2007; Quinton et al., 2010-), massive sequestration of POC upstream of dams
significantly alters the nature and flux of downstream POC (Syvitski et al., 2022; Maavara et al., 2017; Best et al., 2019;
Battin et al., 2009).

75 Even though recent research has advanced our understanding on the governing environmental factors from catchment- to
global scales (Galy et al., 2015; Hilton, 2008; Coppola et al., 2018; Hemingway et al., 2019; Eglinton et al., 2021), there is
still a lack of quantitative constraints on the effect of environmental drivers on the carbon isotopic composition of riverine
POC. The recent release of the International Soil Radiocarbon Database (ISRaD) (Lawrence et al., 2020) enables to improve
Earth system models aiming to predict global SOC radiocarbon distribution and turnover time (Shi et al., 2020; Carvalhais et
80 al., 2014). However, such prediction is still hampered for fluvial POC, despite existing capabilities for modeling water
discharge, SPM concentration, and POC content based on global water quality datasets (Ittekkot, 1988; Ludwig et al., 1996,
Meybeck, 1993), such as the WBMsed global hydrology model (Cohen et al., 2014) or the Global NEWS2 (Mayorga et al.,
2010). **Recently, owing to the improved water quality datasets, other sophisticated river biogeochemistry models have been**
built to understand riverine carbon cycling and environmental inturbations, such as the regional process-based Dynamic In-
85 **Stream Chemistry module (DISC-CARBON), but still focus on different carbon fluxes (van Hoek et al., 2021).**

Here we provide a new database for riverine POC, called MOREPOC (for MODern River archivEs of Particulate Organic
Carbon) v1.10, compiling ~~2,018-283~~ $\Delta^{14}\text{C}$ data, thereby representing a significant update of the previously reported global
dataset by Marwick et al. (2015) with 531 ~~reported $\Delta^{14}\text{C}$ measurements~~ $\Delta^{14}\text{C}$ -data. MOREPOC v1.01, featuring data published
in international, peer-reviewed articles, provides the basis to 1) uncover the fundamental mechanisms of preservation and
90 alteration of river POC (in terms of "bulk" POC as well as for the individual POC_{bio} and $\text{POC}_{\text{petro}}$ pools); and 2) help with the
construction of numerical models able to simulate the isotopic compositions of POC in the context of global change.
MOREPOC database is publicly available on the Zenodo repository at
<https://doi.org/10.5281/zenodo.7055970>~~<https://doi.org/10.5281/zenodo.6541925>~~ (Ke et al., 2022).

2. MOREPOC v1.01: a compilation of data on global riverine POC

95 2.1 Data source

In MOREPOC v1.01, through a comprehensive literature investigation of ~~117-115~~ peer-reviewed articles, we compiled 3,424

546 POC-related data entries (each entry represents an individual sample), including 2,100-195 with SPM concentration, 2,9433,053 with POC content, 3,260-402 with stable carbon isotope $\delta^{13}\text{C}$ values, 2,018-283 with radiocarbon activity $\Delta^{14}\text{C}$ values, 1,835-937 with total nitrogen content (see details in Table.1), and 309-299 with aluminum to silicon mass ratios (Al/Si). In addition, reported analytical uncertainties for POC content, $\delta^{13}\text{C}$, and $\Delta^{14}\text{C}$ are included in MOREPOC. Note that river-bed or bank sediments are not included in this database. We selected studies reporting at least one carbon isotopic data, and those with paired elemental and dual carbon isotopic values. Studies reporting only POC contents were not compiled into the MOREPOC v1.01. ~~Error-Potential mistake~~ generated during the compilation of data entries was carefully checked ~~through manual and statistical examination~~, and duplicate data were removed. A supplementary table “MOREPOC_RM” is provided to give additional information on references, sampling method of SPM, filtration strategy, ~~decarbonization-carbonate removal~~ methods, and detailed information for ~~the types of acid used to remove carbonateacid-adopted~~, etc.

Table 1: Riverine SPM data availability for each continent.

Continent	Samples no.	SPM no.	POC no.	TN no.	$\delta^{13}\text{C}$ no.	$\Delta^{14}\text{C}$ no.
Asia	1,889954	1,131159	1,793849	1,106166	1,811897	1,186361
Africa	278291	277290	277290	103	278291	115
Europe	130	81	99	23	125	113
Oceania	91	59	91	89	91	26
North America	756793	336365	424460	379411	676712	475558
South America	280287	216241	259264	135	279286	103110
Total	3,424546	2,100195	2,9433,053 53	1,8351,937 37	3,260402	2,018283

2.2 Georeferencing

~~When available, sampling location was~~ Location of samples was digitalized if available, and an associate ArcGIS data layer in shapefile format (see MOREPOC_v1.1.rar) is provided with all points projected in a Geographic Coordinate System using the World Geodetic System 1984 (WGS1984). For references only providing a sampling map without any numerical information on sampling location, sampling coordinates were manually extracted using ArcGIS 10.3 after georeferenced adjustment. In the end, 3,211-339 SPM samples have coordinate information among the 3,424-546 compiled SPM entries (Figure 1). Furthermore, it can be noted that most studies chose sampling locations where SPM can be taken as representative ~~the average level~~ of biogeochemical processes ~~of~~ at catchment scale, *i.e.*, the river mouth, to better understand the compositions, transport behavior, and fluxes of POC either going to a confluence or an estuary (*e.g.*, Bouchez et al., 2014; Hilton et al., 2015; Holmes et al., 2022).

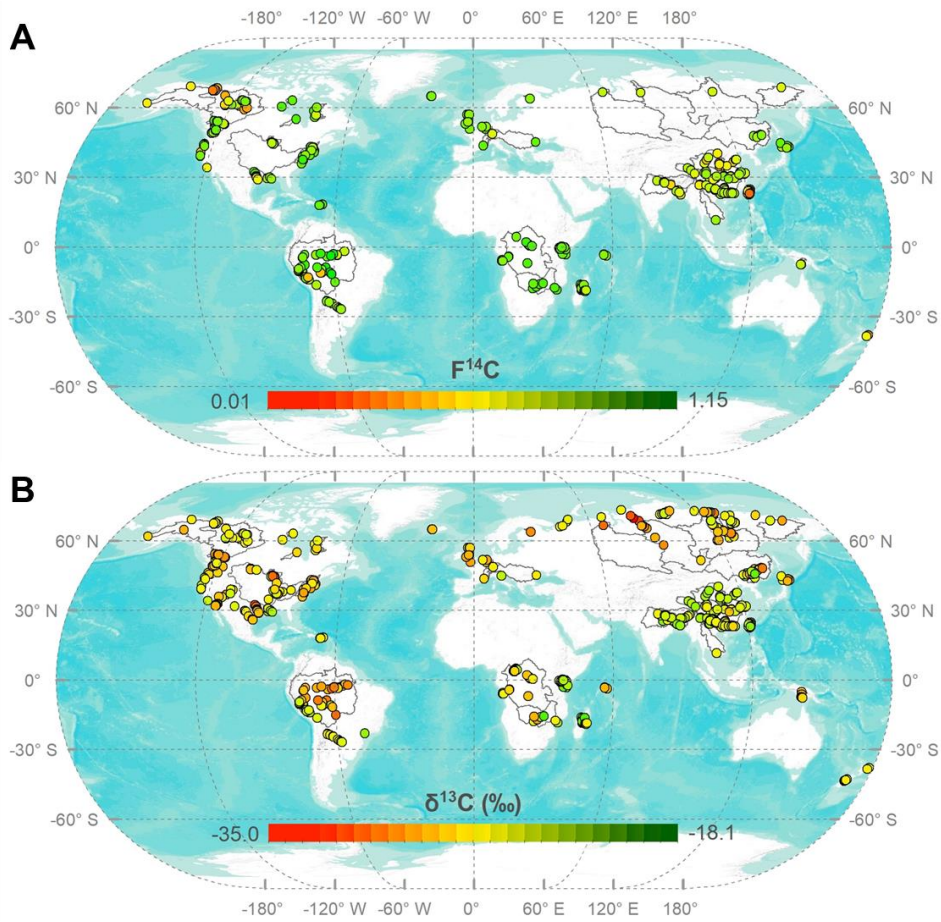


Figure 1: Overview of the dual carbon isotope data of MOREPOC v1.01. A; $Fm^{14}C$ values; B : $\delta^{13}C$ values. Note that an average value is presented when several samples have been collected at the same location.

2.3 Database structure

To make MOREPOC v1.0-1 machine-readable, the compiled parameters were labeled with a short name as shown in Table. 2.

Table. 2 Description of the parameters of the MOREPOC v1.0-1 database.

Parameter	Description	MOREPOC column name
River name	Name of the major river basin	rivbas _naid
Sub river name	Name of the sampled river/stream	basriv_naid
Country	Name of country or places	country
Continent	Name of the continent	cont
Sampling site/code	Expedition sampling ID	code
Sampling date	Time (month/day/year) when the SPM sample was collected	time_m/d/y
Latitude	Decimal latitude using WGS 1984	lat
Longitude	Decimal longitude using WGS 1984	lon
Sampling technique	Method of SPM sampling	type_spm
Size fraction of SPM	Reported size fractions analyzed	fra_spm
SPM concentration (mg/L)	The total dry weight of SPM in mg per liter water column	conc_spm
POC concentration (mg/L)	The total dry weight of POC in mg per liter water column	conc_poc
POC content (%)	The total POC content of SPM in wt %	perc_poc
POC content uncertainty (1σ)	The analytical uncertainty for POC content (1σ)	perc_poc_1sd
$\delta^{13}\text{C}$ (‰)	$\delta^{13}\text{C}$ values of POC (decarbonated carbonate removed) in ‰	d13e d13C_poc
$\delta^{13}\text{C}$ uncertainty (1σ)	The analytical uncertainty for $\delta^{13}\text{C}$ of POC	d13C_1sd
$\Delta^{14}\text{C}$ (‰)	$\Delta^{14}\text{C}$ values of POC (decarbonated carbonate removed) in ‰	D14e D14C_poc
$\Delta^{14}\text{C}$ uncertainty (1σ)	The analytical uncertainty for $\Delta^{14}\text{C}$ of POC	D14C_1sd
Fraction modern (Fm)	Fraction modern of POC	f14eF14C
Radiocarbon ages (year)	Radiocarbon ages before present (1950)	Reage_14C
TN content (%)	The total nitrogen content of SPM in wt %	perc_tn
C _{org} /N mass ratio	Mass- The mass ratio of POC to TN in SPM	cn_marratio
Al/Si mass ratio	Mass- The mass ratio of Al to Si in SPM	asalsi_marratio
Reference	Full list of citations of the data source	ref
Complete reference	Complete information for cited references	ref_c
Measured isotopes parameters	carbon Summarization of ¹³ C or/and ¹⁴ C elemental and isotopic carbon parameters measured	isopara_m
Calculated parameters	Summarization of elemental and isotopic carbon parameters calculated	para_c
Filter	Filter used to obtain SPM	filter
Acid	The acid type used to remove carbonate in SPM	acid
Decarbonization —Carbonate removal method	The method used to remove carbonate in SPM	m_acid

Acid concentration	The concentration of adopted acid to remove carbonate in SPM	conc_acid
Decarbonization —Carbonate removal temperature	The environmental temperature for acid to remove carbonate in SPM	temp_acid
Decarbonization —Carbonate removal duration	The reaction time used for acid to remove carbonate in SPM	time_acid
Note	Additional information for the-carbonate removal decarbonization process	note

2.4 Information on sampling technique

In the compiled studies, five different sampling techniques (parameter "type_spm" of MOREPOC v1.01) have been adopted to retrieve river sediments with the aim of measuring POC content and composition:

- *Surface SPM sampling ("type_spm = SS")* consists in collecting SPM within the first meter below the channel surface. This sampling scheme is the most frequently used and widely adopted in riverine POC studies.
- *Mid-depth SPM sampling ("MS")* consists in collecting SPM at an intermediate depth between the river surface and bottom. This sampling strategy has been used in studies on the Mekong (Martin et al., 2013) and the Mackenzie (Campeau et al., 2020).
- *Integrated sampling over depth profiles ("ISD")* aims at obtaining a representative SPM sample accounting for grain size sorting along the water column, typically by making a flux-weighted composite of several samples collected at different depths along the water column. This sampling strategy has been adopted only for the Huanghe and the Changjiang (Wang et al., 2012), and for the Zengjiang, a tributary of the Zhujiang (Gao et al., 2007).
- *Point sampling along depth profiles ("PSD")* is the collection of SPM along individual depth profiles at different depths in the water columns. In this method and in contrast to the previous one, each SPM sample is treated and analyzed separately. This method allows accessing the full range of particle sizes of SPM, explaining its wide use in the literature (e.g., Ganges-Brahmaputra [Galy et al., 2008a, b], Mackenzie [Hilton et al., 2015], Bermejo [Repasch et al., 2021]).
- *Point sampling over transects ("PST")* corresponds to PSD collection of SPM along several depth profiles across a given river channel section. This sophisticated sampling scheme allows for the exploration of the potential lateral heterogeneity in a river channel. It has been recently used in the Amazon (Bouchez et al., 2014), the Salween and the Irrawaddy (Baronas et al., 2020), and the Danube (Freymond et al., 2018).

2.5 Information on SPM extraction from river water samples and on analysed size fractions

Broadly speaking, two methods are commonly adopted to extract SPM from a water sample, 1) continuous flow centrifugation, whereby large volumes of water can be centrifuged at high centrifugal forces; 2) filtration under pressure or vacuum using membranes made of glass fiber (GF/F), PolyEtherSulfone (PES), Polycarbonate (PTCE), Nylon, quartz fiber, or Mixed Cellulose Esters (MCE), at a porosity mesh size of ranging from 0.2 μm to 1.0 μm . This information is recorded in MOREPOC_RM in detail if described in the corresponding source reference (parameter "Filters").

In general, most studies used bulk SPM retrieved after filtration for the analysis of POC. However, in some studies, only certain size fractions of SPM were analyzed, after separation into *e.g.*, a fine (<63 µm) and a coarse (>63 µm) fraction. This information is reported in MOREPOC v1.0-1 as the “fra_spm” parameter (see Table 2).

2.6 Information on ~~decarbonization~~ carbonate removal method

Particulate inorganic carbon (PIC) and POC have distinct carbon isotopic signatures, such that the accuracy of POC $\delta^{13}\text{C}$ and $\Delta^{14}\text{C}$ values could be compromised if the PIC is not efficiently removed by acidification prior to POC analysis (Komada et al., 2008). ~~Two-Three~~ methods have been ~~mostly adopted~~ adopted in the studies referenced in MOREPOC v1.01:

- The “acid rinse method”, in which sediment samples are ~~acidified~~ soaked with diluted acid at a given temperature for a given time, and then rinsed with distilled water.
- The “acid vapor method”, in which sediment samples are exposed to vaporous concentrated hydrochloric acid in a closed system maintained at a given temperature for a given time, and then evacuated under vacuum.
- The “acid infiltration method”, in which sediment samples are infiltrated in-situ in silver capsules with diluted hydrochloric acid, and then subjected to drying.

The “acid rinse method” and “acid vapor method” have been widely used by the community to remove carbonates from sediments, the “acid infiltration method” is also a common carbonate-removal method but is only reported by Menges et al., 2020 in MOREPOC v1.1.

In addition, a separate file of MOREPOC v1.0-1 (“MOREPOC_RM”) provides detail on carbonate removal ~~decarbonization~~ method (*m_acid*), acid type (*acid*), molarity and quality (*conc_acid*), reaction time in unit of hours (*time_acid*), and reaction temperature in Celsius degrees (*temp_acid*), allowing for quality evaluation of the method used in the cited references.

2.7 Definitions of POC composition variables and units

In MOREPOC v1.01, all data are either taken directly from references or calculated from the reference data. POC content (POC%), and total nitrogen content (TN%) are reported as dry weight percentage (%). Besides, POC concentration in river water (mg/L) can be calculated using SPM concentration reported as dry weight per liter (mg/L) and percentage content of POC (%).

Most importantly, the fundamental component of MOREPOC v1.0-1 consists ~~in~~ of an extensive dataset for stable carbon isotope values ($\delta^{13}\text{C}$, in ‰ relative to VPDB) and radiocarbon compositions (provided as both $\Delta^{14}\text{C}$ in ‰ or as $F^{14}\text{C}$; see below). Fraction modern, $F^{14}\text{C}$, is the deviation of a sample’s ^{14}C atoms from that of the modern standard. Conventional Radiocarbon Ages (RCA) are given in MOREPOC v1.0-1 following Stuiver and Polach (1977), using the Libby half-life of 5,567 years with the mean life of 8,033 for ^{14}C . RCA is expressed in units of years before present (BP), with year zero being 1950⁰:

$$\text{RCA} = -8033 \ln (F^{14}\text{C}) \quad (1)$$

$\Delta^{14}\text{C}$ value, which is defined as the relative difference between the absolute international standard (the base year 1950) and sample activity corrected for age and mass-dependent fractionation (Stuiver and Polach, 1977), is reported in MOREPOC v1.0-1 as well. A positive $\Delta^{14}\text{C}$ indicates the presence of "bomb carbon", whereas a negative $\Delta^{14}\text{C}$ indicates that the radioactive decay of C overwhelms any incorporation of bomb carbon into the sample. The $\Delta^{14}\text{C}$ calculation is defined as equation 2:

$$\Delta^{14}\text{C} \text{ (in ‰)} = \left[F^{14}\text{C} * \exp\left(\frac{1950-yr}{8267}\right) - 1 \right] * 1000 \quad (2)$$

Where *yr* is the year when the sediment was collected, 8,267 is the true mean life of ^{14}C using the Cambridge half-life of 5,730 years.

The term fraction of modern ($F^{14}\text{C}$) is adopted in the above equations, $F^{14}\text{C}$ is defined as equation 3 (Donahue et al., 1990):

$$F^{14}\text{C} = \frac{\left(\frac{^{14}\text{C}}{^{13}\text{C}}\right)_{\text{sample}[-25]}}{0.95 \left(\frac{^{14}\text{C}}{^{13}\text{C}}\right)_{\text{OxI}[-19]}} \quad (3)$$

Where the denominator is 95% of the ^{14}C activity of the Oxalic Acid I (OxI) standard material in 1950, and the numerator is corrected for fractionation to a common $\delta^{13}\text{C}$ value of -25‰.

Lastly, if available, the aluminum-to-silicon mass ratio (Al/Si) is also provided in MOREPOC v1.0-1. This elemental ratio is an efficient proxy for the particle size of riverine sediment, allowing to characterize the grain size effect of sediments on POC loading in fluvial delivery (Bouchez et al., 2011; Galy et al., 2007/2008b; Bouchez et al., 2011; Hilton et al., 2015). The mineralogy and particle size of sediments are generally related, with coarse particles being quartz-rich (low Al/Si ratios) and fine particles being clay-rich (high Al/Si ratios) (Galy et al., 2008b). POC contents are usually positively correlated with proportions of fine-grained fractions (Mayer, 1994; Galy et al., 2008b; Bouchez et al., 2014).

2.8 Extent of MOREPOC v1.0-1

Although MOREPOC v1.0-1 features data from river systems worldwide, it does not offer the same degree of representativeness for all the continents with, for instance, an over-representation of Asian rivers and an under-representation of rivers draining Europe and Oceania (Table. 1). It can be noticed that there are relatively abundant POC studies in North America fluvial systems. However, MOREPOC database also indicates the lack of studies on POC in fluvial systems in the cryosphere regions such as Antarctica and Greenland as well as in arid regions, including Australia, and vast areas spanning from northern Africa to middle east Asia (Figure 1).

MOREPOC v1.0-1 database does not compile elemental and dual isotopic compositions of molecular compounds (plant-wax fatty-acid and lignin-phenol), thermal labile fractions, or black carbon. However, such complementary data could be incorporated into future versions.

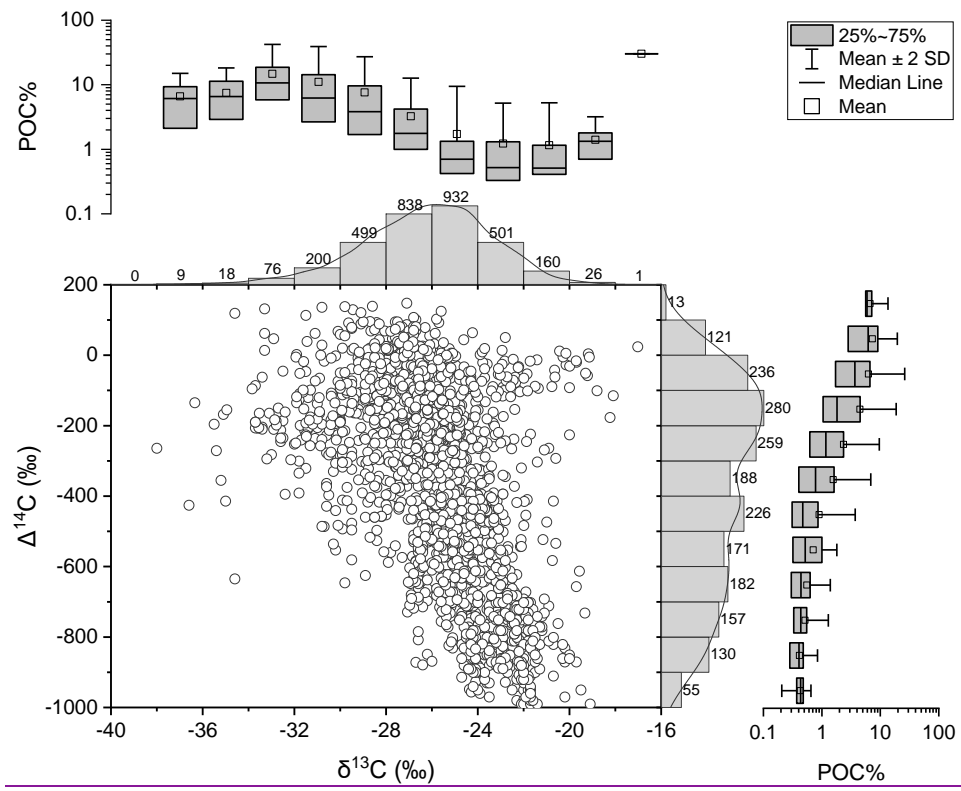
210 3. Global riverine POC patterns

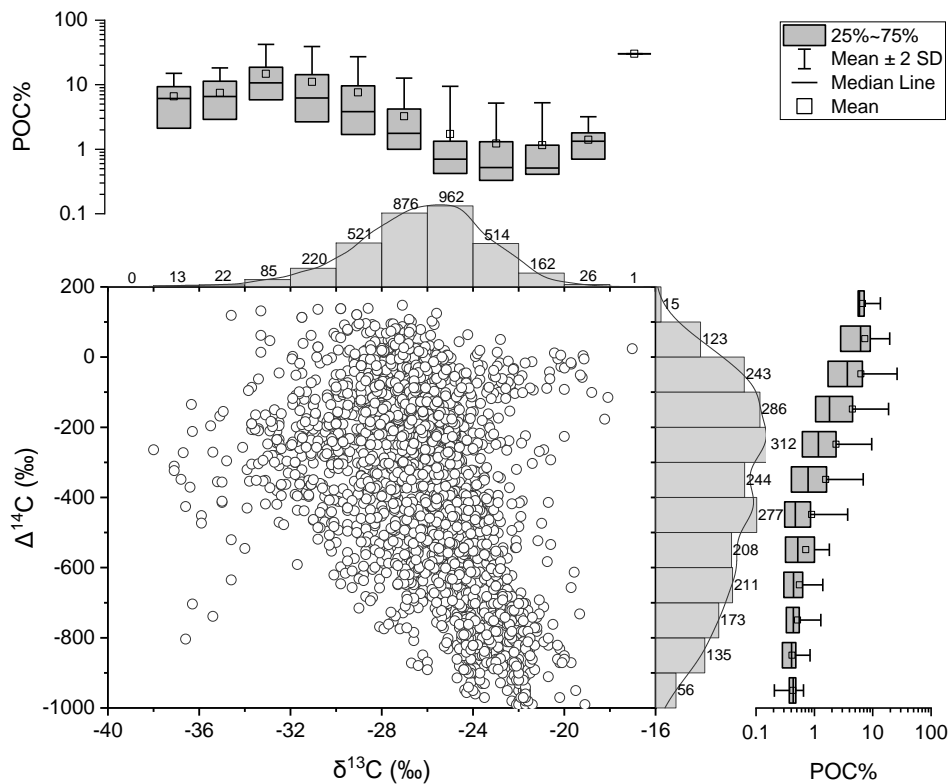
3.1 Trends of $\delta^{13}\text{C}$ and $\Delta^{14}\text{C}$ in MOREPOC v1.01

The mobilization of terrestrial organic matter into fluvial systems depends on the interplay between tectonics, climate, geomorphology, lithology, and anthropogenic activities, all controlling to some extent the amount and composition of riverine POC (Blair and Leithold, 2010; Eglinton et al., 2021).

215 Riverine POC displays significant heterogeneity in elemental and isotopic compositions of carbon around the globe (Figures 1 and 2). $\delta^{13}\text{C}$ values (n=3,244,402) range from -38‰ to -17‰ with an average value of -26.23‰. As shown in Figure 2, the majority of the data falls between -28‰ and -24‰ (n=1,759,770, 54.252.0% of total entries), which is consistent with the overall isotopic signature of the terrestrial biosphere of $-26\pm 7\%$ (Schidlowski et al., 1988). The age of riverine POC spans from "modern" (that is, recording bomb-derived carbon) to "ancient" (strongly influenced by fossil petrogenic source), with $\Delta^{14}\text{C}$ values (n=2,018,283) ranging from -990.1‰ to 147.7‰ with a statistical average of -380.36‰. A large fraction of the $\Delta^{14}\text{C}$ values (n=775, 38.433.9% of total entries) falls within the range -300‰ to 0‰, this range dominates the database in Marwick et al (2015) as well (n=278, 52.3% of Marwick's total entries). The MOREPOC v1.0-1 dataset is on average more ^{14}C depleted than that of Marwick et al (2015).

225 Around the globe, the most ancient POC ($\Delta^{14}\text{C} = -990\%$) is found in small mountainous rivers in Taiwan (Hilton et al., 2010), in which the entirety of POC is derived from the erosion of sedimentary rocks. In the riverine POC dataset of MOREPOC v1.01, bomb carbon signals are abundant ($\Delta^{14}\text{C} > 0\%$), particularly for African rivers in tropical regions such as Athi-Galana-Sabaki, Tana, Zambezi, and Congo (Marwick et al., 2015; Spencer et al., 2012); rivers in North America including Hudson, Siuslaw, and York; rivers draining to the Hudson Bay (Leithold et al., 2006; Raymond and Bauer, 2001; Godin et al., 2017; Longworth et al., 2007); and the Andean Amazon (Mayorga et al., 2005; Townsend-Small et al., 2007). Around the Qinghai-Tibet Plateau, where most large river systems in eastern and southern Asia share similar high elevation source regions, POC is usually characterized by relatively depleted ^{14}C signals due to high erosion rates of sedimentary rocks in mountainous regions, like in the Ganges-Brahmaputra (Galy et al., 2007) or the Changjiang (Wang et al., 2012; Wang et al., 2019), etc., and erosion of soils containing pre-aged OC, e.g. Huanghe (Tao et al., 2015). The most depleted ^{13}C signatures (less than -35‰) are observed for POC from Arctic rivers, such as the Ob', Yukon, and Kolyma (Holmes et al., 2022). The highest $\delta^{13}\text{C}$ values (higher than -22‰) are found in rivers from-in Africa (Athi-Galana-Sabaki, Betsiboka, and Tana; Marwick et al., 2015; Tamooh et al., 2013) and mountainous rivers (e.g., Taiwan [Hilton et al., 2010], upper Ganges [Galy et al., 2007; Galy et al., 2008b], Minjiang [Wang et al., 2019, etc.]; ~~Hilton et al., 2010; Galy et al., 2007; Galy et al., 2008b; Wang et al., 2019~~).





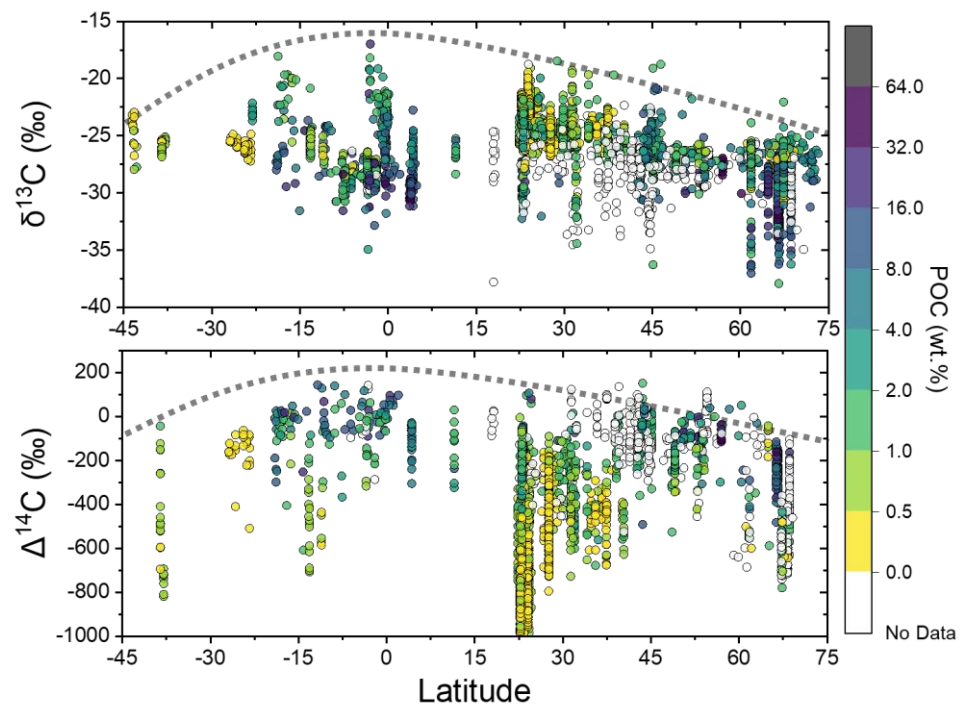
240 **Figure 2:** $\delta^{13}\text{C}$ versus $\Delta^{14}\text{C}$ of MOREPOC v1.0-1 ($n=12,860,129$). Frequency distribution histograms for $\delta^{13}\text{C}$ (x-axis) and $\Delta^{14}\text{C}$ (y-axis) are shown, with $\delta^{13}\text{C}$ values binned every -2.5% from -40% to -15% , and $\Delta^{14}\text{C}$ values binned every -50% from -1000% to 200% . Each bin is labeled with the number of samples it hosts. Solid lines represent the corresponding probability density functions. Box charts represent the statistical analysis of POC% in each bine of $\delta^{13}\text{C}$ (x-axis) and $\Delta^{14}\text{C}$ (y-axis).

245 As observed in the global compilation in Figure 2, elemental and isotopic data of POC generally show an inverse relationship between $\delta^{13}\text{C}$ and $\Delta^{14}\text{C}$, and generally an increasing POC content with higher radiocarbon activity of POC. Indeed, OC from sedimentary rocks (*i.e.*, dead OC with $\Delta^{14}\text{C}=-1000\%$ by definition) usually has ^{13}C -enriched signatures compared to recent biomass. Eroded material from sedimentary rocks thus has lower POC content, is ^{14}C -depleted signatures and has relatively high $\delta^{13}\text{C}$ signatures. This global pattern stems from the global dominance of C3 plants in the studied-compiled catchments (Figure 2). However, it can also be observed that POC-rich riverine SPM can also be relatively enriched at-in ^{13}C , *i.e.*, $\delta^{13}\text{C}$ values larger than -20% (Figure 2 and Figure 3). This pattern indicates the presence of an additional pool of ^{14}C - and ^{13}C -rich POC in the terrestrial environment (Cerling et al., 1997), consisting of modern C4-plants in catchments dominated by grasslands or savannah (*e.g.*, Marwick et al., 2015). The maximum values of $\delta^{13}\text{C}$ and $\Delta^{14}\text{C}$ of POC (dotted line in Figure 3) tend to be more depleted at high latitudes than at low latitudes. This might reflect the combined effects of increasing coverage of C4 plants in tropical regions and the input of pre-aged OC_{bio} from degrading permafrost at high latitude (Cerling et al., 1997; Still et al., 2003)-the major POC components: 1) dominated by POC_{bio} , the combined effects of increasing coverage of C4 plants in tropical regions and the input of pre-aged OC_{bio} of C3 plants from degrading permafrost at high latitude (Cerling et

250

255

al., 1997; Still et al., 2003); 2) dominated by $\text{POC}_{\text{petro}}$, rivers in mountainous regions tends to erode ^{13}C -enrich petrogenic OC (Hilton et al., 2010; Galy et al., 2007). In addition, aquatic authigenic production can be an important mechanism contributing ^{13}C -depleted and ^{14}C -enriched POC (Longworth et al., 2007; Marwick et al., 2015; Wu et al., 2018).



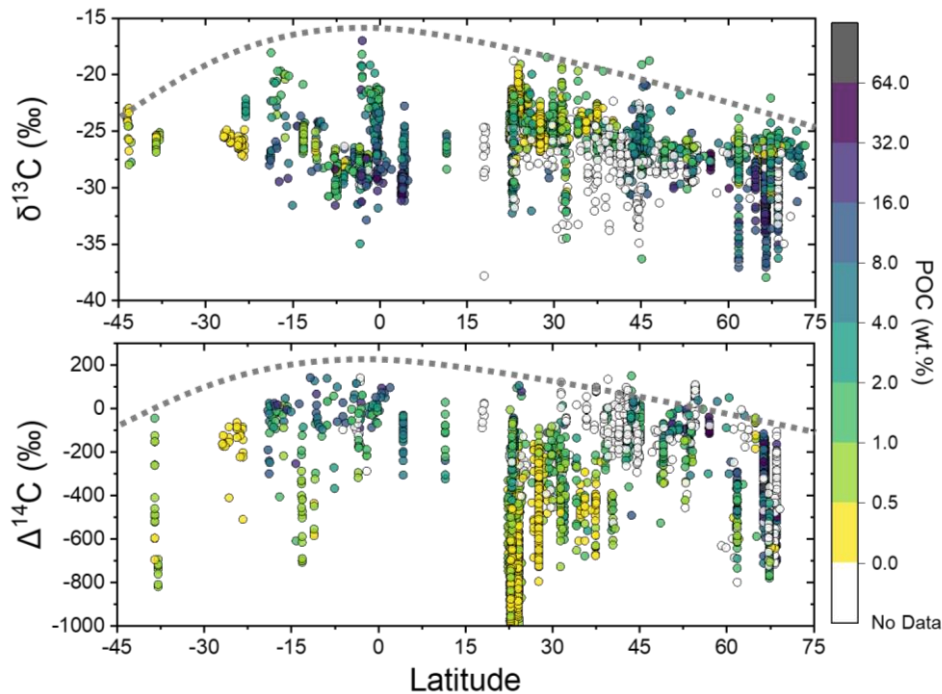


Figure 3: Latitudinal trends in $\delta^{13}\text{C}$ (n=3,064,204) and $\Delta^{14}\text{C}$ (n=1,944,212) in MOREPOC v1.01. Colors indicate POC content (wt. %). Dotted lines represent upper envelopes of $\delta^{13}\text{C}$ and $\Delta^{14}\text{C}$ values of POC.

3.2 Relationships between riverine SPM and POC

265 MOREPOC v1.0-1 features data from rivers with SPM concentrations ranging from 0.35 to 199,000 mg/L ~~and with POC~~
~~concentration-content~~ from 0.01% to 91.67%. SPM and POC concentrations (both expressed in mg/L; n=2,044,115) are
 positively correlated (Figure 4). However, the global trend shows that an increase in SPM concentration is accompanied by a
 decrease in POC content (in %), which is largely owing to a dilution effect by inorganic materials (Figure 4, Ittekkot, 1998;
 Ludwig et al., 1996; Meybeck, 1993). In MOREPOC v1.01, large SPM concentrations (over 10,000 mg/L) are generally
 270 observed in mountainous rivers, such as the Choshui and Liwu rivers in Taiwan (Hilton et al., 2008; Kao et al., 2014), the
 Santa Clara River (USA) (Masiello and Druffel, 2001), or the Minjiang (a major tributary of the upper Changjiang, China)
 (Wang et al., 2019). The Huanghe is an exception in that it has very large SPM concentrations in its middle reaches where it
 drains the Chinese Loess Plateau (Qu et al., 2020; Hu et al., 2015). Although the sediment of highly turbid rivers is typically
 POC-poor, high sediment concentrations generate the largest POC export rates (Figure 4). This observation also underlines
 275 the importance of sediment transport near the channel bottom in large rivers where SPM concentration is usually much higher
 than at the surface (Figure 5, e.g., Ganges-Brahmaputra-Meghna [Galy et al 2007, 2008b], Mackenzie [Hilton et al., 2015],
 Amazon [Bouchez et al., 2014], and Yukon (Holmes et al., 2022) etc.), as well as the role of stochastic events leading to high-
 turbidity episodes such as storms, landslides, or earthquakes (Hilton et al., 2008; Wang et al., 2015; Frith et al., 2018). Small
 SPM concentrations (less than 10 mg/L) are ~~characteristic of~~ generally found in rivers during the frozen season or rivers

draining either high-latitude or tropical areas characterized by low-relief settings, in which typical POC content is relatively high (Gao et al., 2007; Holmes et al., 2022).

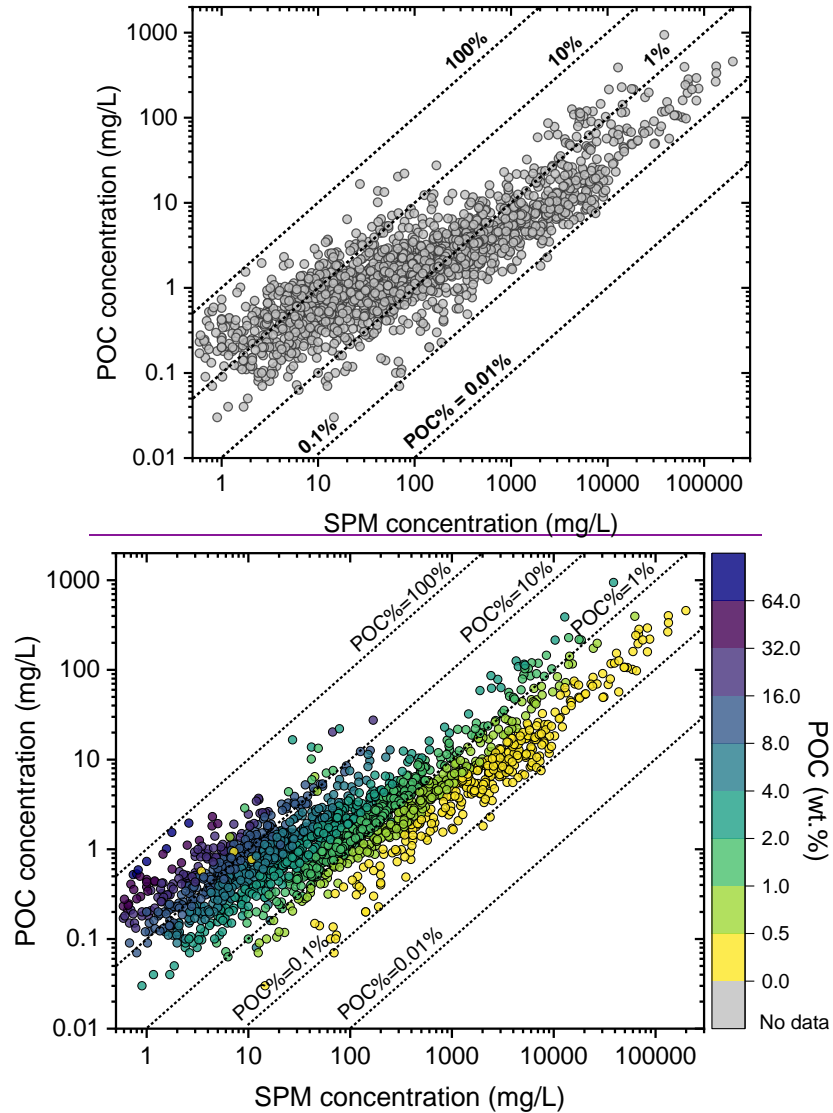


Figure 4: River SPM concentration vs. POC concentration ($n=2,041,135$), both expressed in mg/L. Dotted lines represent contours of constant POC content. Colors indicate the POC content from data entries in MOREPOC v1.1.

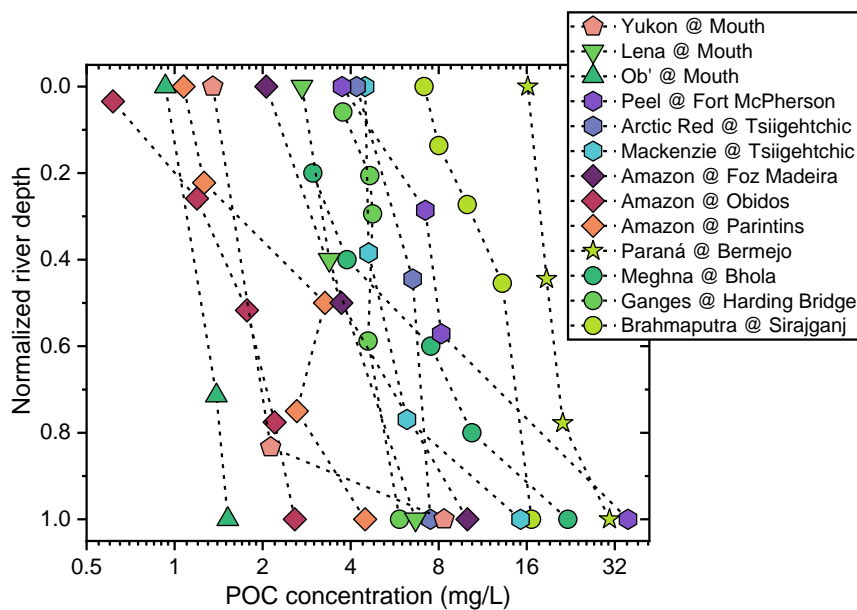
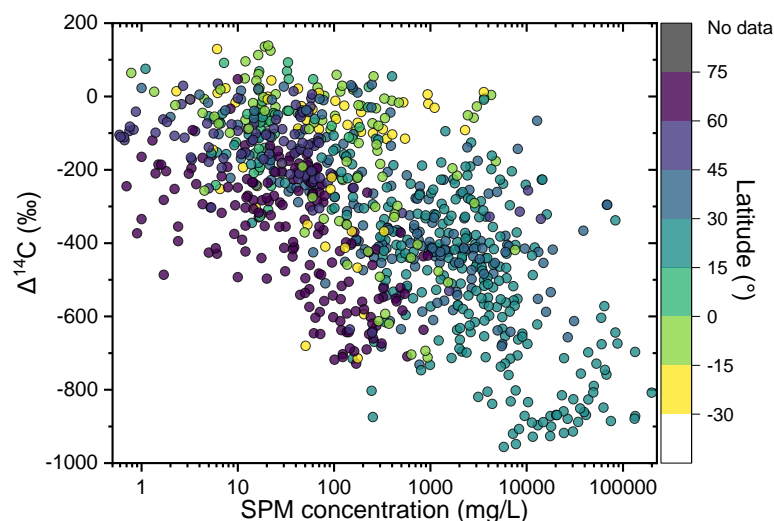


Figure 5: POC concentration variation in vertical water columns from depth profiles in global large rivers. Selected depth profiles are from the Yukon, Lena, and Ob' (Holmes et al., 2022), Mackenzie including Peel and Arctic Red (Hilton et al., 2015), Amazon (Bouchez et al., 2014), Paraná (Repasch et al., 2021), and Ganges-Brahmaputra-Meghna systems (Galy et al., 2007, 2008b). Normalized river depth is calculated by normalizing the individual sample depth to the maximum sample depth of the corresponding profile.

Globally In general, POC becomes ^{14}C -depleted with increasing suspended sediment load (Figure 5) and decreasing POC content. (Figure 6). These relationships patterns are most likely caused by the dilution of POC_{bio} by $\text{POC}_{\text{petro}}$ in areas of strong erosion (Leithold et al., 2016). However, MOREPOC v1.1 also shows new observations highlights that low concentrated SPM load associated with high POC content is often characterized by significantly low $\Delta^{14}\text{C}$ values (Figure 5, 6, 7). Most of those samples come from Arctic river systems. This rises some concerns because Arctic permafrost soils store approximately twice the current amount of carbon contained in the currently is in Earth's atmosphere (Zimov et al., 2006), and biospheric OC that was previously stored in frozen soils over thousands of years is being released and can induce accelerated environmental changes (Schuur et al., 2015; Vonk et al., 2015; Wild et al., 2019). How OC in permafrost regions responds to global warming should be a key research issue in future studies. Meanwhile, it is worth to note, for a given SPM concentration, a large range of ^{14}C composition abundance can be observed. For example, rivers draining low-latitude, tropical regions (especially $10^{\circ}\text{N} - 10^{\circ}\text{S}$; e.g., African rivers) or high-latitude regions ($60^{\circ}\text{N} - 75^{\circ}\text{N}$; e.g., Siberian Arctic rivers) are usually characterized by relatively low SPM concentration and abundant POC composition. However, in general, But Nevertheless, riverine POC from the low-latitude African rivers is much younger compared to that from the Arctic Siberian regions. This difference most likely stems from the contrasting radiocarbon activities and turnover time of the soil organic carbon (SOC) between these two regions, which are primarily driven by climate (Eglinton et al., 2021; Marwick et al., 2015; Wild et al., 2019; Vonk et al., 2015).

The MOREPOC v1.0-1 dataset also reveals that under a given climate, river systems can be heterogeneous in terms of SPM

310 concentration and associated POC composition. For example, amongst circum-Arctic rivers, the Mackenzie River has a relatively large SPM concentration of ~~462~~-135.1 mg/L on average ($1\sigma=16.6$, $n=118106$) with ~~2.43~~0.1% POC ($1\sigma=0.39$, $n=109105$) characterized by a fairly low $\Delta^{14}\text{C}$ (average value of ~~-599.5~~%, $1\sigma=7.7$, $n=118$) near the river mouth; (Hilton et al., 2015; Schwab et al., 2020; Holmes et al., 2022; ~~Campeau et al., 2020~~). In contrast, the Yenisei River only has an average SPM concentration of ~~5.27~~ mg/L ($1\sigma=0.6$, $n=8386$) but much higher POC contents (~~17.418~~0.0%, $1\sigma=2.1$, $n=8483$) and $\Delta^{14}\text{C}$ values (~~-264342.3~~%, $1\sigma=15.7$, $n=2766$; Holmes et al., 2022). Such difference suggests that lithology and geomorphology can play
315 an important role in riverine POC composition and load by providing a substantial fraction of fossil OC (Hilton et al., 2015). On the other hand, small mountainous rivers such as those in Taiwan or those draining the Himalayas show large SPM concentrations and low POC contents with low radiocarbon activities. These regions characterized by active tectonics, steep slopes, and intense precipitation, act as global hotspots for sediment production and thus petrogenic OC mobilization (Milliman and Farnsworth, 2011; Hilton and West, 2020).



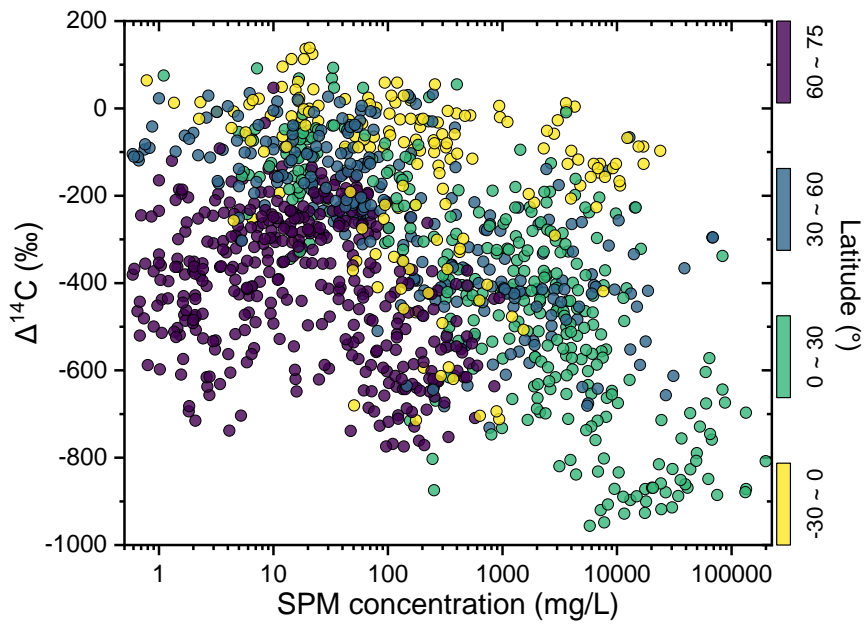
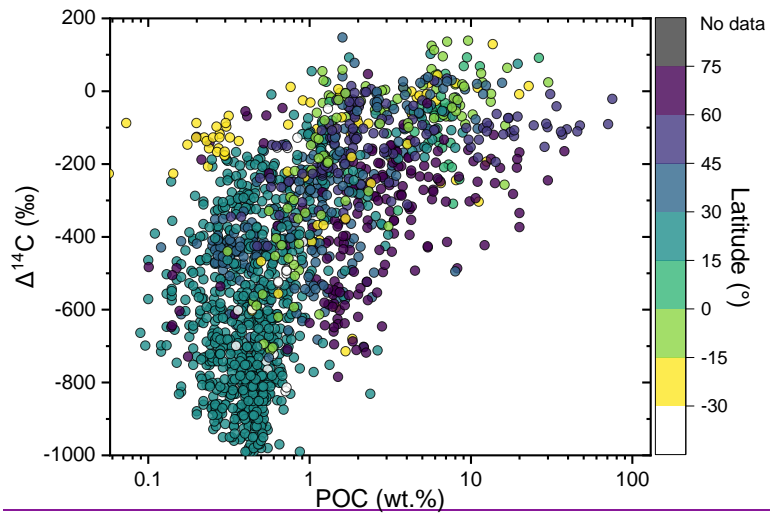


Figure 56: POC $\Delta^{14}\text{C}$ vs. SPM concentration (n=9431157). Colors indicate the latitude of the sampling location. Note the log-scale used for SPM concentration.



325

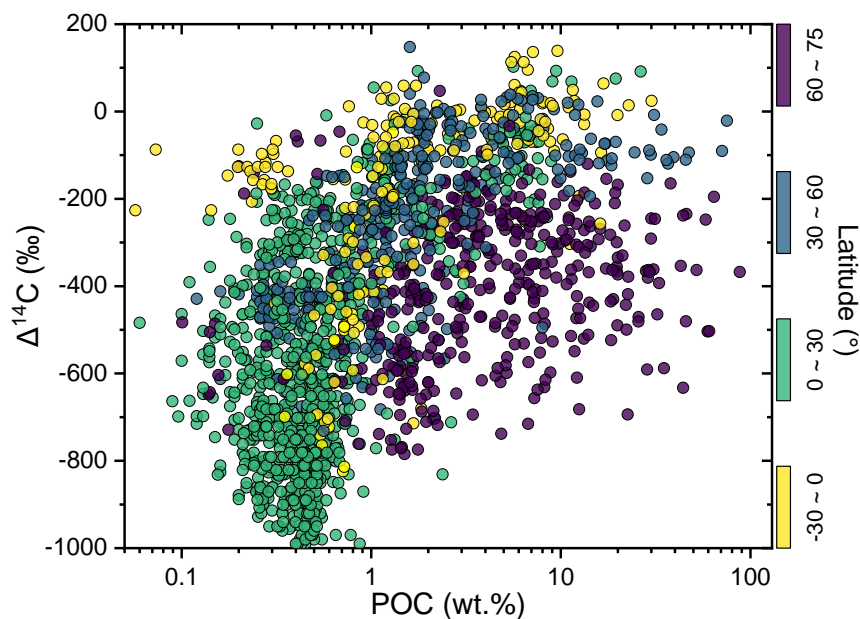


Figure 67: $\Delta^{14}\text{C}$ values vs. POC content (n=1,649,860). Colors indicate the latitude of the sampling location. Note the **log scale** used for POC content.

4. Database availability

MOREPOC v1.0-1 database is publicly available on the Zenodo repository in machine-readable formats as Excel spreadsheet (.xlsx), comma limited table (.csv), and GIS shapefile at <https://doi.org/10.5281/zenodo.7055970> <https://doi.org/10.5281/zenodo.6541925> (Ke et al., 2022).

5. Conclusions

In this paper, we introduce MOREPOC, the largest and most comprehensive database for riverine suspended particulate matter (SPM) concentration and particulate organic carbon (POC) composition, including POC and total nitrogen (TN) content, stable carbon isotope (¹³C), cosmogenic-radioactive carbon isotope (¹⁴C), as well as aluminum-to-silicon (Al/Si) mass ratios. MOREPOC will benefit the scientific community carrying out research on riverine POC sources, transport, and fate ~~as well as Earth system modelers~~. Furthermore, it will help feed and validate Earth system models in order to improve the ability of models to constrain all the components of the global carbon cycle. Combined with ocean sediment databases, such as CASCADE (Circum-Arctic Sediment Carbon DatabasE, Martens et al., 2021) or MOSAIC (Modern Ocean Sediment Archive and Inventory of Carbon, Van der Voort et al., 2021), MOREPOC will enable a better understanding of the fate of POC from the terrestrial source to sink at the ocean bottom. Existing environmental raster global datasets for climate, geomorphology, lithology, tectonics, hydrology, and land use, also offer promising prospects for the use of MOREPOC for identifying the

controls on POC fluxes and composition, in particular using advanced statistical analysis or machine learning techniques.
345 Future updates of MOREPOC should include new bulk POC parameters as well as data on molecular fractions, thermal labile fractions, or specific components such as black carbon or fossil carbon, which should, in turn, provide additional insight into the alteration of riverine POC from source to sink, an essential feature of the global carbon cycle.

Author contribution

350 YK collected the MOREPOC data and conceptualized, designed, structured, and filled the database. YK and DC contributed to the database checking. YK prepared the manuscript. YK drafted and coordinated the manuscript with input from DC, JB, and CQ.

Competing interests

The authors declare that they have no conflict of interest.

Acknowledgments

355 The development of MOREPOC database was funded by the Agence Nationale de la Recherche (ANR) SEDIMAN (Grant ANR-15-CE01-0012), the authors acknowledge the Ph.D. scholarship awarded to Yutian Ke (No. 201706180008) by the China Scholarship Council.

Financial support

360 This research has been supported by Agence Nationale de la Recherche (ANR) SEDIMAN (Grant ANR-15-CE01-0012) and the China Scholarship Council (Grant 201706180008).

Reference

- Baronas, J. J., Stevenson, E. I., Hackney, C. R., Darby, S. E., Bickle, M. J., Hilton, R. G., Larkin, C. S., Parsons, D. R., Khaing, A. M., and Tipper, E. T.: Integrating suspended sediment flux in large alluvial river channels: application of a synoptic Rouse-based model to the Irrawaddy and Salween rivers., *J. Geophys. Res.*, 125, <https://doi.org/10.1029/2020JF005554>, 2020.
- 365 Battin, T. J., Luysaert, S., Kaplan, L. A., Aufdenkampe, A. K., Richter, A., and Tranvik, L. J.: The boundless carbon cycle, *Nat. Geosci.*, 2, 598–600, <https://doi.org/10.1038/ngeo618>, 2009.
- Berner, R. A.: The long-term carbon cycle, fossil fuels and atmospheric composition, *Nature*, 426, 323–326, <https://doi.org/10.1038/nature02131>, 2003.

- Best, J.: Anthropogenic stresses on the world's big rivers, *Nat. Geosci.*, 12, 7–21, <https://doi.org/10.1038/s41561-018-0262-x>, 2019.
- Blair, N. E. and Aller, R. C.: The fate of terrestrial organic carbon in the marine environment., *Ann. Rev. Mar. Sci.*, 4, 401–423, <https://doi.org/10.1146/annurev-marine-120709-142717>, 2012.
- Blair, N. E., Leithold, E. L., and Aller, R. C.: From bedrock to burial: the evolution of particulate organic carbon across coupled watershed-continental margin systems, *Mar. Chem.*, 92, 141–156, <https://doi.org/10.1016/j.marchem.2004.06.023>, 2004.
- Blair, N. E., Leithold, E. L., Ford, S. T., Peeler, K. A., Holmes, J. C., and Perkey, D. W.: The persistence of memory: The fate of ancient sedimentary organic carbon in a modern sedimentary system, *Geochim. Cosmochim. Acta*, 67, 63-73, [https://doi.org/10.1016/S0016-7037\(02\)01043-8](https://doi.org/10.1016/S0016-7037(02)01043-8), 2003.
- Bouchez, J., Gaillardet, J., France-Lanord, C., Maurice, L., and Dutra-maia, P.: Grain size control of river suspended sediment geochemistry: Clues from Amazon River depth profiles, *Geochemistry Geophys. Geosystems*, 12, <https://doi.org/10.1029/2010GC003380>, 2011.
- Bouchez, J., Galy, V., Hilton, R. G., Gaillardet, J., Moreira-Turcq, P., Pérez, M. A., France-Lanord, C., and Maurice, L.: Source, transport and fluxes of Amazon River particulate organic carbon: Insights from river sediment depth-profiles, *Geochim. Cosmochim. Acta*, 133, 280–298, 2014.
- Burdige, D. J.: Burial of terrestrial organic matter in marine sediments: A re-assessment, *Global Biogeochem Cycles*, 19, n/a-n/a, <https://doi.org/10.1029/2004gb002368>, 2005.**
- Campeau, A., Soerensen, A. L., Martma, T., Åkerblom, S., and Zdanowicz, C.: Controls on the ¹⁴C content of dissolved and particulate organic carbon mobilized across the Mackenzie River basin, Canada, *Global Biogeochem. Cycles*, 34, e2020GB006671, <https://doi.org/10.1029/2020GB006671>, 2020.
- Carvalhais, N., Forkel, M., Khomik, M., Bellarby, J., Jung, M., Migliavacca, M., Saatchi, S., Santoro, M., Thurner, M., and Weber, U.: Global covariation of carbon turnover times with climate in terrestrial ecosystems, *Nature*, 514, 213–217, <https://doi.org/10.1038/nature13731>, 2014.
- Cerling, T. E., Harris, J. M., MacFadden, B. J., Leakey, M. G., Quade, J., Eisenmann, V., and Ehleringer, J. R.: Global vegetation change through the Miocene/Pliocene boundary, *Nature*, 389, 153–158, <https://doi.org/10.1038/38229>, 1997.
- Cohen, S., Kettner, A. J., and Syvitski, J. P. M.: Global suspended sediment and water discharge dynamics between 1960 and 2010: Continental trends and intra-basin sensitivity, *Glob. Planet. Change*, 115, 44–58, <https://doi.org/10.1016/j.gloplacha.2014.01.011>, 2014.
- Coppola, A. I., Wiedemeier, D. B., Galy, V., Haghypour, N., Hanke, U. M., Nascimento, G. S., Usman, M., Blattmann, T. M., Reisser, M., Freymond, C. V., Zhao, M. X., Voss, B., Wacker, L., Schefuß, E., Peucker-Ehrenrink, B., Abiven, Samuel., Schmidt, M. W., and Eglinton, T. I.: Global-scale evidence for the refractory nature of riverine black carbon, *Nat. Geosci.*, 11(8), 584-588, <https://doi.org/10.1038/s41561-018-0159-8>, 2019.
- Dethier, E. N., Renshaw, C. E., and Magilligan, F. J.: Rapid changes to global river suspended sediment flux by humans, *Science*, 376, 1447–1452, <https://doi.org/10.1126/science.abn7980>, 2022.**

Donahue, D. J., T. W. Linick, and A. J. T. Jull.: Isotope-Ratio and Background Corrections for Accelerator Mass Spectrometry Radiocarbon Measurements, *Radiocarbon.*, 32(2): 135–42, <https://doi.org/10.1017/S0033822200040121>, 1990.

405 Eglinton, T. I., Galy, V. V., Hemingway, J. D., Feng, X., Bao, H., Blattmann, T. M., Dickens, A. F., Gies, H., Giosan, L., and Haghypour, N.: Climate control on terrestrial biospheric carbon turnover, *Proc. Natl. Acad. Sci.*, 118, <https://doi.org/10.1073/pnas.2011585118>, 2021.

Freymond, C. V., Lupker, M., Peterse, F., Haghypour, N., Wacker, L., Filip, F., Giosan, L., and Eglinton, T. I.: Constraining Instantaneous Fluxes and Integrated Compositions of Fluvially Discharged Organic Matter, *Geochemistry Geophys. Geosystems*, 19, 2453–2462, <https://doi.org/10.1029/2018GC007539>, 2018.

410 Frith, N. V., Hilton, R. G., Howarth, J. D., Gröcke, D. R., Fitzsimons, S. J., Croissant, T., Wang, J., McClymont, E. L., Dahl, J., and Densmore, A. L.: Carbon export from mountain forests enhanced by earthquake-triggered landslides over millennia, 11(10), 772–776, *Nature Geoscience*, <https://doi.org/10.1038/s41561-018-0216-3>, 2018.

Galy, V., France-Lanord, C., Beyssac, O., Faure, P., Kudrass, H., and Palhol, F.: Efficient organic carbon burial in the Bengal fan sustained by the Himalayan erosional system., *Nature*, 450, 407–410, <https://doi.org/10.1038/nature06273>, 2007.

Galy, V., Beyssac, O., France-Lanord, C., and Eglinton, T.: Recycling of Graphite During Himalayan Erosion: A Geological Stabilization of Carbon in the Crust, *Science (80-.)*, 322, 943–945, <https://doi.org/10.1126/science.1161408>, 2008a.

Galy, V., France-Lanord, C., and Lartiges, B.: Loading and fate of particulate organic carbon from the Himalaya to the Ganga–Brahmaputra delta, *Geochim. Cosmochim. Acta*, 72, 1767–1787, <https://doi.org/10.1016/j.gca.2008.01.027>, 2008b.

420 Galy, V. and Eglinton, T.: Protracted storage of biospheric carbon in the Ganges-Brahmaputra basin, *Nat. Geosci.*, 4, 843–847, <https://doi.org/10.1038/ngeo1293>, 2011.

Galy, V., Peucker-Ehrenbrink, B., and Eglinton, T. I.: Global carbon export from the terrestrial biosphere controlled by erosion, *Nature*, 521, 204–207, <https://doi.org/10.1038/nature14400>, 2015.

425 Gao, Q., Tao, Z., Yao, G., Ding, J., Liu, Z., and Liu, K.: Elemental and isotopic signatures of particulate organic carbon in the Zengjiang River, southern China, *Hydrol. Process. An Int. J.*, 21, 1318–1327, <https://doi.org/10.1002/hyp.6358>, 2007.

Godin, P., Macdonald, R. W., Kuzyk, Z. Z. A., Goñi, M. A., and Stern, G. A.: Organic matter compositions of rivers draining into Hudson Bay: Present-day trends and potential as recorders of future climate change, *J. Geophys. Res. Biogeosciences*, 122, 1848–1869, <https://doi.org/10.1002/2016JG003569>, 2017.

430 Hemingway, J. D., Rothman, D. H., Grant, K. E., Rosengard, S. Z., Eglinton, T. I., Derry, L. A., and Galy, V. V.: Mineral protection regulates long-term global preservation of natural organic carbon, *Nature*, 570, 228–231, <https://doi.org/10.1038/s41586-019-1280-6>, 2019.

Hilton, R. G. and West, A. J.: Mountains, erosion and the carbon cycle, *Nat. Rev. Earth Environ.*, 1, 284–299, <https://doi.org/10.1038/s43017-020-0058-6>, 2020.

435 Hilton, R. G., Galy, A., Hovius, N., Chen, M.-C., Horng, M.-J., and Chen, H.: Tropical-cyclone-driven erosion of the terrestrial biosphere from mountains, *Nat. Geosci.*, 1, 759–762, <https://doi.org/10.1038/ngeo333>, 2008.

Hilton, R. G., Galy, A., Hovius, N., Horng, M.-J., and Chen, H.: Efficient transport of fossil organic carbon to the ocean by

- steep mountain rivers: An orogenic carbon sequestration mechanism, *Geology*, 39, 71–74, <https://doi.org/10.1130/G31352.1>, 2011.
- Hilton, R. G., Gaillardet, J., Calmels, D., and Birck, J.-L.: Geological respiration of a mountain belt revealed by the trace element rhenium, *Earth Planet. Sci. Lett.*, 403, 27–36, <https://doi.org/10.1016/j.epsl.2014.06.021>, 2014.
- Hilton, R. G., Galy, V., Gaillardet, J., Dellinger, M., Bryant, C., O'Regan, M., Gröcke, D. R., Coxall, H., Bouchez, J., and Calmels, D.: Erosion of organic carbon in the Arctic as a geological carbon dioxide sink, *Nature*, 524, 84–87, <https://doi.org/10.1038/nature14653>, 2015.
- Holmes, R.M., J.W. McClelland, S.E. Tank, R.G.M. Spencer, and A.I. Shiklomanov. Arctic Great Rivers Observatory. Water Quality Dataset, Version 20220609. <https://www.arcticgreatrivers.org/data>, 2022.
- Hu, B., Li, J., Bi, N., Wang, H., Wei, H., Zhao, J., Xie, L., Zou, L., Cui, R., Li, S., Liu, M., and Li, G.: Effect of human-controlled hydrological regime on the source, transport, and flux of particulate organic carbon from the lower Huanghe (Yellow River), *Earth Surf. Process. Landforms*, 40, 1029–1042, <https://doi.org/10.1002/esp.3702>, 2015.
- Ittekkot, V.: Global trends in the nature of organic matter in river suspensions, *Nature*, 332, 436–438, 1988.
- Kao, S.-J., Hilton, R. G., Selvaraj, K., Dai, M., Zehetner, F., Huang, J.-C., Hsu, S.-C., Sparkes, R., Liu, J. T., and Lee, T.-Y.: Preservation of terrestrial organic carbon in marine sediments offshore Taiwan: mountain building and atmospheric carbon dioxide sequestration, *Earth Surf. Dyn.*, 2, 127–139, <https://doi.org/10.5194/esurf-2-127-2014>, 2014.
- Ke, Y. T., Calmels, D., Bouchez, J., Cécile, Q.: MOdern River archivEs of Particulate Organic Carbon: MOREPOC, Dataset version 1.1, Zenodo [dataset], <https://doi.org/10.5281/zenodo.7052190>~~<https://doi.org/10.5281/zenodo.6541925>~~.
- Komada, T., Anderson, M. R., and Dorfmeier, C. L.: Carbonate removal from coastal sediments for the determination of organic carbon and its isotopic signatures, $\delta^{13}\text{C}$ and $\Delta^{14}\text{C}$: comparison of fumigation and direct acidification by hydrochloric acid, *Limnol. Oceanogr. Methods*, 6, 254–262, <https://doi.org/10.4319/lom.2008.6.254>, 2008.
- Lawrence, C. R., Beem-Miller, J., Hoyt, A. M., Monroe, G., Sierra, C. A., Stoner, S., Heckman, K., Blankinship, J. C., Crow, S. E., and McNicol, G.: An open-source database for the synthesis of soil radiocarbon data: International Soil Radiocarbon Database (ISRaD) version 1.0, *Earth Syst. Sci. Data*, 12, 61–76, <https://doi.org/10.5194/essd-12-61-2020>, 2020.
- Leithold, E. L., Blair, N. E., and Perkey, D. W.: Geomorphologic controls on the age of particulate organic carbon from small mountainous and upland rivers, *Global Biogeochem. Cycles*, 20, <https://doi.org/10.1029/2005GB002677>, 2006.
- Leithold, E. L., Blair, N. E., and Wegmann, K. W.: Source-to-sink sedimentary systems and global carbon burial: A river runs through it, *Earth-Science Rev.*, 153, 30–42, <https://doi.org/10.1016/j.earscirev.2015.10.011>, 2016.
- Longworth, B. E., Petsch, S. T., Raymond, P. A., and Bauer, J. E.: Linking lithology and land use to sources of dissolved and particulate organic matter in headwaters of a temperate, passive-margin river system, *Geochim. Cosmochim. Acta*, 71, 4233–4250, <https://doi.org/10.1016/j.gca.2007.06.056>, 2007.
- Ludwig, W., Probst, J.-L., and Kempe, S.: Predicting the oceanic input of organic carbon by continental erosion, *Global Biogeochem. Cycles*, 10, 23–41, <https://doi.org/10.1029/95GB02925>, 1996.
- Maavara, T., Lauerwald, R., Regnier, P., and Van Cappellen, P.: Global perturbation of organic carbon cycling by river

damming, *Nat Commun*, 8, 15347, <https://doi.org/10.1038/ncomms15347>, 2017.

Martens, J., Romankevich, E., Semiletov, I., Wild, B., Van Dongen, B., Vonk, J., Tesi, T., Shakhova, N., Dudarev, O. V, and Kosmach, D.: CASCADE-The Circum-Arctic Sediment Carbon Database, *Earth Syst. Sci. Data*, 13, 2561-2572, <https://doi.org/10.5194/essd-13-2561-2021>, 2021.

475 Martin, E. E., Ingalls, A. E., Richey, J. E., Keil, R. G., Santos, G. M., Truxal, L. T., Alin, S. R., and Druffel, E. R. M.: Age of riverine carbon suggests rapid export of terrestrial primary production in tropics, *Geophys. Res. Lett.*, 40, 5687–5691, <https://doi.org/10.1002/2013GL057450>, 2013.

Marwick, T. R., Tamooh, F., Teodoru, C. R., Borges, A. V, Darchambeau, F., and Bouillon, S.: The age of river transported carbon: A global perspective, *Global Biogeochem. Cycles*, 29, 122-137, <https://doi.org/10.1002/2014GB004911>, 2015.

480 Masiello, C. A. and Druffel, E. R. M.: Carbon isotope geochemistry of the Santa Clara River, *Global Biogeochem. Cycles*, 15, 407–416, 2001.

Masiello, C. A. and Druffel, E. R. M.: Carbon isotope geochemistry of the Santa Clara River, *Global Biogeochem. Cycles*, 15, 407–416, <https://doi.org/10.1029/2000GB001290>, 2001.

485 Mayer, L. M.: Surface area control of organic carbon accumulation in continental shelf sediments, *Geochim. Cosmochim. Acta*, 58, 1271–1284, [https://doi.org/10.1016/0016-7037\(94\)90381-6](https://doi.org/10.1016/0016-7037(94)90381-6), 1994.

Mayorga, E., Aufdenkampe, A. K., Masiello, C. A., Krusche, A. V, Hedges, J. I., Quay, P. D., Richey, J. E., and Brown, T. A.: Young organic matter as a source of carbon dioxide outgassing from Amazonian rivers, *Nature*, 436, 538–541, <https://doi.org/10.1038/nature03880>, 2005.

490 Mayorga, E., Seitzinger, S. P., Harrison, J. A., Dumont, E., Beusen, A. H. W., Bouwman, A. F., Fekete, B. M., Kroeze, C., and Van Drecht, G.: Global nutrient export from WaterSheds 2 (NEWS 2): model development and implementation, *Environ. Model. Softw.*, 25, 837–853, <https://doi.org/10.1016/j.envsoft.2010.01.007>, 2010.

Meybeck, M.: Riverine transport of atmospheric carbon: sources, global typology and budget, *Water. Air. Soil Pollut.*, 70, 443–463, <https://doi.org/10.1007/BF01105015>, 1993.

495 Milliman, J. D. and Farnsworth, K. L.: River discharge to the coastal ocean: a global synthesis, Cambridge University Press, 2011.

Montgomery, D. R.: Soil erosion and agricultural sustainability, *Proc. Natl. Acad. Sci.*, 104, 13268–13272, <https://doi.org/10.1073/pnas.0611508104>, 2007.

Petsch, S. T.: Weathering of organic carbon: Treatise on Geochemistry, v. 12, 2014.

500 Qu, Y., Jin, Z., Wang, J., Wang, Y., Xiao, J., Gou, L., Zhang, F., Liu, C., Gao, Y., Suarez, M. B., and Xu, X.: The sources and seasonal fluxes of particulate organic carbon in the Yellow River, *Earth Surf. Process. Landforms*, 45, 2004–2019, <https://doi.org/10.1002/esp.4861>, 2020.

Quinton, J. N., Govers, G., Van Oost, K., and Bardgett, R. D.: The impact of agricultural soil erosion on biogeochemical cycling, *Nat. Geosci.*, 3, 311–314, <https://doi.org/10.1038/ngeo838>, 2010.

Raymond, P. A. and Bauer, J. E.: Riverine export of aged terrestrial organic matter to the North Atlantic Ocean, *Nature*, 409,

- 497–500, <https://doi.org/10.1038/35054034>, 2001.
- Repasch, M., Scheingross, J. S., Hovius, N., Lupker, M., Wittmann, H., Haghypour, N., Gröcke, D. R., Orfeo, O., Eglinton, T. I., and Sachse, D.: Fluvial organic carbon cycling regulated by sediment transit time and mineral protection, *Nat. Geosci.*, 14, 842–848, <https://doi.org/10.1038/s41561-021-00845-7>, 2021.
- Schidlowski, M.: A 3,800-million-year isotopic record of life from carbon in sedimentary rocks, *Nature*, 333, 313–318, <https://doi.org/10.1038/333313a0>, 1988.
- Shi, Z., Allison, S. D., He, Y., Levine, P. A., Hoyt, A. M., Beem-Miller, J., Zhu, Q., Wieder, W. R., Trumbore, S., and Randerson, J. T.: The age distribution of global soil carbon inferred from radiocarbon measurements, *Nat. Geosci.*, 13, 555–559, <https://doi.org/10.1038/s41561-020-0596-z>, 2020.
- Scheingross, J. S., Repasch, M. N., Hovius, N., Sachse, D., Lupker, M., Fuchs, M., Halevy, I., Gröcke, D. R., Golombek, N. Y., Haghypour, N., Eglinton, T. I., Orfeo, O., and Schleicher, A. M.: The fate of fluvially-deposited organic carbon during transient floodplain storage, *Earth and Planetary Science Letters*, 561, 116822, <https://doi.org/10.1016/j.epsl.2021.116822>, 2021.
- Schuur, E. A., McGuire, A. D., Schadel, C., Grosse, G., Harden, J. W., Hayes, D. J., Hugelius, G., Koven, C. D., Kuhry, P., Lawrence, D. M., Natali, S. M., Olefeldt, D., Romanovsky, V. E., Schaefer, K., Turetsky, M. R., Treat, C. C., and Vonk, J. E.: Climate change and the permafrost carbon feedback, *Nature*, 520, 171–9, <https://doi.org/10.1038/nature14338>, 2015.
- Stallard, R. F.: Terrestrial sedimentation and the carbon cycle: Coupling weathering and erosion to carbon burial, *Global Biogeochem. Cycles*, 12, 231–257, <https://doi.org/10.1029/98GB00741>, 1998.
- Spencer, R. G. M., Hernes, P. J., Aufdenkampe, A. K., Baker, A., Gulliver, P., Stubbins, A., Aiken, G. R., Dyda, R. Y., Butler, K. D., and Mwamba, V. L.: An initial investigation into the organic matter biogeochemistry of the Congo River, *Geochim. Cosmochim. Acta*, 84, 614–627, <https://doi.org/10.1016/j.gca.2012.01.013>, 2012.
- Still, C. J., Berry, J. A., Collatz, G. J., and DeFries, R. S.: Global distribution of C3 and C4 vegetation: carbon cycle implications, *Global Biogeochem. Cycles*, 17, 1–6, <https://doi.org/10.1029/2001GB001807>, 2003.
- Stuiver, M. and Polach, H. A.: Discussion reporting of ¹⁴C data, *Radiocarbon*, 19, 355–363, <https://doi.org/10.1017/S0033822200003672>, 1977.
- Syvitski, J., Ángel, J. R., Saito, Y., Overeem, I., Vörösmarty, C. J., Wang, H., and Olago, D.: Earth’s sediment cycle during the Anthropocene, *Nat Rev Earth Environ*, 3, 179–196, <https://doi.org/10.1038/s43017-021-00253-w>, 2022.
- Tamooh, F., Borges, A. V., Meysman, F. J. R., Van den Meersche, K., Dehairs, F., Merckx, R., and Bouillon, S.: Dynamics of dissolved inorganic carbon and aquatic metabolism in the Tana River basin, Kenya, 10, 6911–6928, <https://doi.org/10.5194/bg-10-6911-2013>, 2013.
- Tao, S., Eglinton, T. I., Montluçon, D. B., McIntyre, C., and Zhao, M.: Pre-aged soil organic carbon as a major component of the Yellow River suspended load: Regional significance and global relevance, *Earth Planet. Sci. Lett.*, 414, 77–86, <https://doi.org/10.1016/j.epsl.2015.01.004>, 2015.
- Townsend-Small, A., Noguera, J. L., McClain, M. E., and Brandes, J. A.: Radiocarbon and stable isotope geochemistry of

- organic matter in the Amazon headwaters, Peruvian Andes, *Global Biogeochem. Cycles*, 21, <https://doi.org/10.1029/2006GB002835>, 2007.
- 540 van der Voort, T. S., Blattmann, T. M., Usman, M., Montluçon, D., Loeffler, T., Tavagna, M. L., Gruber, N., and Eglinton, T. I.: MOSAIC (Modern Ocean Sediment Archive and Inventory of Carbon): a (radio) carbon-centric database for seafloor surficial sediments, *Earth Syst. Sci. Data*, 13, 2135–2146, <https://doi.org/10.5194/essd-13-2135-2021>, 2021.
- 545 van Hoek, W. J., Wang, J., Vilmin, L., Beusen, A. H. W., Mogollón, J. M., Müller, G., Pika, P. A., Liu, X., Langeveld, J. J., Bouwman, A. F., and Middelburg, J. J.: Exploring Spatially Explicit Changes in Carbon Budgets of Global River Basins during the 20th Century, *Environ. Sci. Technol.*, 55, 16757–16769, <https://doi.org/10.1021/acs.est.1c04605>, 2021.
- Vonk, J. E., Tank, S. E., Bowden, W. B., Laurion, I., Vincent, W. F., Alekseychik, P., Amyot, M., Billet, M. F., Canário, J., and Cory, R. M.: Reviews and syntheses: Effects of permafrost thaw on Arctic aquatic ecosystems, 12, 7129–7167, <https://doi.org/10.5194/bg-12-7129-2015>, 2015.
- 550 Wacker, L., Bonani, G., Friedrich, M., Hajdas, I., Kromer, B., Němec, M., Ruff, M., Suter, M., Synal, H.-A., and Vockenhuber, C.: MICADAS: routine and high-precision radiocarbon dating, *Radiocarbon*, 52, 252–262, <https://doi.org/10.1017/S0033822200045288>, 2010.
- 555 Wild, B., Andersson, A., Bröder, L., Vonk, J., Hugelius, G., McClelland, J. W., Song, W., Raymond, P. A., and Gustafsson, Ö.: Rivers across the Siberian Arctic unearth the patterns of carbon release from thawing permafrost, *Proc. Natl. Acad. Sci.*, 116, 10280–10285, <https://doi.org/10.1073/pnas.1811797116>, 2019.
- Wang, X., Ma, H., Li, R., Song, Z., and Wu, J.: Seasonal fluxes and source variation of organic carbon transported by two major Chinese Rivers: The Yellow River and Changjiang (Yangtze) River, *Global Biogeochem. Cycles*, 26, <https://doi.org/10.1029/2011gb004130>, 2012.
- 560 Wang, J., Jin, Z., Hilton, R. G., Zhang, F., Densmore, A. L., Li, G., and West, A. J.: Controls on fluvial evacuation of sediment from earthquake-triggered landslides, *Geology*, 43, 115–118, <https://doi.org/10.1130/g36157.1>, 2015.
- Wang, J., Hilton, R. G., Jin, Z., Zhang, F., Densmore, A. L., Gröcke, D. R., Xu, X., Li, G., and West, A. J.: The isotopic composition and fluxes of particulate organic carbon exported from the eastern margin of the Tibetan Plateau, *Geochim. Cosmochim. Acta*, 252, 1–15. <https://doi.org/10.1016/j.gca.2019.02.031>, 2019.
- 565 Wu, Y., Eglinton, T. I., Zhang, J., and Montluçon, D. B.: Spatiotemporal Variation of the Quality, Origin, and Age of Particulate Organic Matter Transported by the Yangtze River (Changjiang), *J. Geophys. Res.*, 123, 2908–2921, <https://doi.org/10.1029/2017JG004285>, 2018.
- Zimov, S. A., Schuur, E. A. G., and Chapin, F. S.: Permafrost and the Global Carbon Budget, *Science*, 312, 1612–1613, <https://doi.org/10.1126/science.1128908>, 2006.